Bimolecular Hole Transfer from the Trimethoxybenzene Radical Cation in the Excited State

Xichen Cai, Mamoru Fujitsuka, and Tetsuro Majima*

The Institute of Scientific and Industrial Research (SANKEN), Osaka University, Mihogaoka 8-1, Ibaraki, Osaka 567-0047, Japan

Received: January 23, 2007; In Final Form: March 3, 2007

Bimolecular hole transfer quenching of the 1,3,5-trimethoxybenzene radical cation ($TMB^{\bullet+}$) in the excited state ($TMB^{\bullet+*}$) by hole quenchers (Q) such as biphenyl (Bp), naphthalene (Np), anisole (An), and benzene (Bz) with higher oxidation potentials than that of TMB was directly observed during the two-color two-laser flash photolysis at room temperature. From the linear relationships between the inverse of the transient absorption changes of $TMB^{\bullet+}$ during the second 532-nm laser excitation versus the inverse of the concentration of Q, the rate constant of the hole transfer from $TMB^{\bullet+*}$ to Q was estimated to be $(8.5 \pm 0.4) \times 10^{10}$, $(1.4 \pm 0.7) \times 10^{11}$, $(1.3 \pm 0.6) \times 10^{11}$, and $(6.4 \pm 0.3) \times 10^{10}$ $M^{-1}s^{-1}$ for Bp, An, Np, and Bz, respectively, in acetonitrile based on the lifetime of $TMB^{\bullet+*}$. The estimated rate constants are larger than the diffusion-controlled rate constant in acetonitrile. Short lifetime, high energy, and high oxidation potential of $TMB^{\bullet+*}$ cause the lifetime-dependent quenching process or static quenching process as the major process during the quenching of $TMB^{\bullet+*}$ by Q as indicated by the Ware's theoretical model. The subsequent hole transfer from $Q^{\bullet+}$ to TMB, giving $TMB^{\bullet+}$, was found to occur at the diffusion-controlled rate for Bp and An as Q. For Q such as Np and Bz, the dimerization of $Q^{\bullet+}$ with Q to give dimer radical cation ($Q_2^{\bullet+}$) occurred competitively with the hole transfer from $Q^{\bullet+}$ to TMB.

Introduction

Organic radical cations and anions are important reactive intermediates in chemistry, physics, and biology. Because of the higher energy of radical ions in the excited states than that in the ground state, higher reactivities of radical ions in the excited states are expected.[1−3] Because the redox potential of radical ions in the excited state is larger than that in the ground state,[3−5] the electron-transfer reaction that cannot occur in the ground state is expected in the excited states.[5,6]

Because of the quite short lifetime of the excited radical, a high concentration of quencher is needed to observe sufficient bimolecular hole- or electron-transfer reaction between the excited radical and quencher in a solution. Under such conditions, the bimolecular reaction rate constant includes dynamic and static quenching terms, of which the latter is lifetime-dependent. Thus, by assuming that the bimolecular reaction proceeds at the diffusion-limiting rate (k_{diff}), one can estimate the lifetime of the excited radicals. On the basis of this assumption, lifetimes of several aromatic radical ions in the excited state have been reported.[7−11] For example, the lifetimes of radical cations in the excited states have been reported to be 120 ps for *cis*-stilbene, 240 ps for *trans*-stilbene,[9] and 450 ps for 1,6-diphenylhexa-1,3,5-triene.[8] The lifetimes of radical anions in the excited states are 1.5 ns for *cis*-stilbene, 2.5 ns for *trans*-stilbene,[10] and approximately 4 ns for dicyanoanthracene, phenazine, and anthraquinones.[11]

It should be emphasized that direct detection of radical ions in the excited state is desired for understanding the properties and reactions of the radical ions in the excited state because the determination of the lifetime of the excited radical by the kinetic analysis of the bimolecular reactions needs assumptions on various important parameters, such as encounter distance and so on. The example of the lifetimes of the excited radicals estimated by direct spectroscopic method is rather limited. The transient absorptions of only a few radical ions in the excited states have been directly measured.[6,12−14] Aromatic imide and diimide radical anions in the excited states have been studied with the subpicosecond transient absorption measurements.[6] The lifetimes of diimide radical anions in the excited states were found to be shorter than 600 ps. The lifetime of the zinc(II) tetraphenylporphine radical cation in the excited states was found to be 17 ps using a combination method of controlled potential coulometry and femtosecond absorption spectrometry.[12] The lifetime of the perylene radical cation in the excited state was found to be 3 ps.[13] Recently, the fluorescence spectrum and 41 ± 2 ps of lifetime corresponding to the $D_2 \rightarrow D_0$ transition of the 1,3,5-trimethoxybenzene radical cation ($TMB^{\bullet+}$) were measured with the ns−ps two-color two-laser flash photolysis in acetonitrile at room temperature.[14] In the case of $TMB^{\bullet+*}$, the lifetime obtained by the direct measurement was shorter than that obtained from the kinetic analysis. This suggests that the rate constant of the hole- and electron-transfer quenching of radical ions in the excited state by quenchers is not equal to k_{diff} but much larger than k_{diff}. Herein, we report the rate constants of the hole transfer from $TMB^{\bullet+*}$ to various quenchers (Q) such as biphenyl (Bp), anisole (An), naphthalene (Np), and benzene (Bz) with higher oxidation potentials than that of TMB based on directly measured $TMB^{\bullet+*}$ lifetime. The subsequent hole transfer from $Q^{\bullet+}$ to TMB is also discussed together with the competitive dimerization of $Q^{\bullet+}$ and Q.

---

* Corresponding author. E-mail: majima@sanken.osaka-u.ac.jp. Tel: +81-6-6879-8495. Fax: +81-6-6879-8499.

10.1021/jp0705626 CCC: $37.00

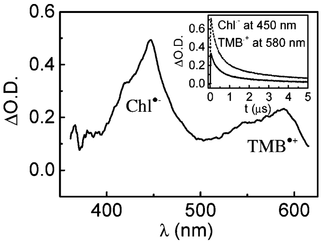

Figure 1. Transient absorption spectra of $TMB^{\bullet+}$ and $Chl^{\bullet-}$ obtained at 100 ns after the 355-nm laser flash during the 355-nm laser irradiation of a mixture of TMB (1.0×10^{-2} M) and Chl (5.0×10^{-3} M) in aerated acetonitrile. The inset shows the decay of $TMB^{\bullet+}$ at 580 nm (solid line) and decay of $Chl^{\bullet-}$ at 450 nm (broken line), respectively.

Experimental Methods

Materials. 1,3,5-Trimethoxybenzene and chloranil were purchased from Aldrich Chem. Co. (purity >99%) and used without further purification. Biphenyl and naphthalene were purchased from Nacalai Tesque Inc. and recrystallized from ethanol before use. Acetonitrile, benzene, and anisole (spectral grade) were purchased from Nacalai Tesque Inc. Sample solutions were freshly prepared in a $1 \times 1 \times 4$ cm^3 rectangular Suprasil cell before irradiation. All experiments were carried out at room temperature.

Two-Color Two-Laser (ns−ns) Flash Photolysis. The two-color two-laser flash photolysis system has been described previously.[15] Briefly, the 355-nm laser flash (10 mJ flash^{-1}) from a Nd:YAG laser (Brilliant, Quantel; 5-ns full width at half-maximum (fwhm)) was used as the first laser to prepare $TMB^{\bullet+}$. The 532-nm laser flash (80 mJ flash^{-1}) from a Nd:YAG laser (Continuum, Surelite II-10; 5-ns fwhm) was used as the second laser to excite $TMB^{\bullet+}$ during the two-color two-laser flash photolysis experiments. Two laser flashes were synchronized by a four-channel digital delay/pulse generator (Stanford Research Systems, Inc., Model DG 535) with a delay time of 10 ns to 10 μs. Two laser flashes with diameters of 0.5 cm were adjusted in the same direction and overlapped through the sample. The probe beam was obtained from a 450 W Xe-lamp (Osram XBO-450). The probe beam was passed through an iris with a diameter of 0.3 cm and sent into the sample with a perpendicular intersection of the laser beams. Additionally, the probe beam was closely arranged to the entrance side of the laser beams. The transmitted probe beam was focused on a monochromator (Nikon G250). The output of the monochromator was monitored using a photomultiplier tube (PMT, Hamamatsu Photonics R928). The signal from the PMT was recorded on a transient digitizer (TDS 580D four-channel digital phosphor oscilloscope, 1 GHz, Tektronix). A Hamamatsu Photonics multichannel analyzer (C5967) system was used for measurement of the transient absorption spectra. The total system was controlled with a personal computer via the GP−IB interface. To avoid any damage of the sample solution by the probe light, a suitable cutoff filter was used in front of the sample. The experiments were repeated at least three times at each concentration of quenchers to obtain the rate constants. The error bar of the rate constant was given based on the averaged results.

Results

Transient Absorption of $TMB^{\bullet+}$. Upon the 355-nm laser irradiation of a mixture of TMB (1.0×10^{-2} M) and chloranil (Chl) (5.0×10^{-3} M) in aerated acetonitrile, Chl was excited to give Chl in the singlet excited state ($^1Chl^*$), which converts rapidly to Chl in the triplet excited state ($^3Chl^*$) with the quantum efficiency of the near unit within 30 ps.[16,17] The electron-transfer reaction occurs between TMB and $^3Chl^*$ to give $TMB^{\bullet+}$ and $Chl^{\bullet-}$.[18,19] The transient absorption spectrum and decay of $TMB^{\bullet+}$ with an absorption peak around 580 nm ($\epsilon = 4000 \pm 500$ M^{-1}cm^{-1})[18,19] are shown in Figure 1.

A part of $Chl^{\bullet-}$ was quenched by oxygen to give $O_2^{\bullet-}$. $TMB^{\bullet+}$ decayed through the charge recombination with $Chl^{\bullet-}$ or $O_2^{\bullet-}$. The reaction mechanism is summarized in eqs 1−6.

$$\mathrm{Chl} + h\upsilon_{355} \rightarrow {}^1\mathrm{Chl}^* \tag{1}$$

$$^1\mathrm{Chl}^* \rightarrow {}^3\mathrm{Chl}^* \tag{2}$$

$$^3\mathrm{Chl}^* + \mathrm{TMB} \rightarrow \mathrm{TMB}^{\bullet+} + \mathrm{Chl}^{\bullet-} \tag{3}$$

$$\mathrm{Chl}^{\bullet-} + \mathrm{O_2} \rightarrow \mathrm{Chl} + \mathrm{O_2}^{\bullet-} \tag{4}$$

$$\mathrm{TMB}^{\bullet+} + \mathrm{Chl}^{\bullet-} \rightarrow \mathrm{TMB} + \mathrm{Chl} \tag{5}$$

$$\mathrm{TMB}^{\bullet+} + \mathrm{O_2}^{\bullet-} \rightarrow \mathrm{TMB} + \mathrm{O_2} \tag{6}$$

Hole Transfer from $TMB^{\bullet+*}$ to Q during the Two-Color Two-Laser Flash Photolysis. Because $Chl^{\bullet-}$ has negligible absorption in the wavelength region longer than 500 nm,[17,20] $TMB^{\bullet+}$ can be selectively excited to $TMB^{\bullet+*}$ during the second 532-nm laser excitation before $TMB^{\bullet+}$ disappears through the charge recombination. Because the lifetime of $TMB^{\bullet+*}$ is 41 ± 2 ps,[14] transient absorption of $TMB^{\bullet+*}$ cannot be measured using the ns−ns two-color two-laser flash photolysis. However, the disappearance of the $TMB^{\bullet+}$ transient absorption was observed in the presence of Q such as Bp, An, Np, and Bz with higher oxidation potentials than that of TMB during the ns−ns two-color two-laser flash photolysis of the mixture of TMB and Chl in aerated acetonitrile.

Bp as Q. The experimental results for the reaction between $TMB^{\bullet+*}$ and Bp are shown in Figure 2. Upon the first 355-nm laser excitation, the rapid growth and decay of the transient absorption around 700 nm was observed in the time scale of 10 and 100 ns, respectively, as shown in Figure 2a. Because the concentration of Bp (0.03 − 0.30 M) was higher than that of TMB (1.0×10^{-2} M), electron transfer from Bp to $^3Chl^*$ occurs to give $Bp^{\bullet+}$ with an absorption peak at 700 nm,[21] which appears as the growth at 700 nm in the 10-ns time scale after the first 355-nm irradiation. Because the oxidation potential of Bp ($E_{1/2}^{ox} = +1.9$ V vs SCE in acetonitrile)[22] is higher than that of TMB ($E_{1/2}^{ox} = +1.5$ V),[22] the subsequent hole transfer from $Bp^{\bullet+}$ to TMB occurs to give $TMB^{\bullet+}$, which appears as the decay at 700 nm in Figure 2a and the growth at 580 nm in Figure 2b in the 100-ns time scale after the first 355-nm irradiation. The reactions are shown as eqs 7 and 8

$$^3\mathrm{Chl}^* + \mathrm{Bp} \rightarrow \mathrm{Bp}^{\bullet+} + \mathrm{Chl}^{\bullet-} \tag{7}$$

$$\mathrm{Bp}^{\bullet+} + \mathrm{TMB} \rightarrow \mathrm{Bp} + \mathrm{TMB}^{\bullet+} \tag{8}$$

During the second 532-nm laser excitation of $TMB^{\bullet+}$, growth and decay of the transient absorption at 700 nm were observed as shown in Figure 2a and the inset. The negative absorption at 700 nm during the second 532-nm laser excitation was attributed to the emission from $TMB^{\bullet+*}$, which decreased with the increasing of the Bp concentration.[18,19] At the same time, the bleaching and complete recovery of the transient absorption of $TMB^{\bullet+}$ at 580 nm were also observed as shown in Figure 2b and the inset. The generation of $Bp^{\bullet+}$ and the bleaching of $TMB^{\bullet+}$ indicate the bimolecular reaction between $TMB^{\bullet+*}$ and

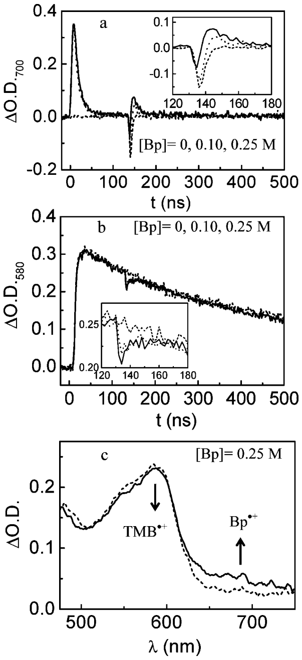

Figure 2. Kinetic traces of ΔO.D.$_{700}$ (a) and ΔO.D.$_{580}$ (b) during the two-color two-laser flash photolysis of a mixture of TMB (1.0×10^{-2} M) and Chl (5.0×10^{-3} M) in aerated acetonitrile in the presence of Bp (0 (dash line), 0.10 (dot line), and 0.25 M (solid line)). The inset shows the profiles expanded during the second 532-nm laser irradiation. Part c shows the spectral changes of TMB$^{\bullet+}$ and Bp$^{\bullet+}$ in the region of 475−750 nm during the one-laser (355-nm laser) (dash line) and two-laser (355-nm laser plus 532-nm laser) (solid line) excitation in the presence of Bp (0.25 M).

Bp during the second 532-nm laser excitation. Because the oxidation potential of TMB$^{\bullet+*}$ is approximately $\sim$+3.5 V from $E_{1/2}{}^{ox}$ of TMB (+1.5 V)[22] and the excitation energy of TMB$^{\bullet+*}$,[18] which is much higher than that of Bp, the bimolecular hole transfer from TMB$^{\bullet+*}$ to Bp to give Bp$^{\bullet+}$ occurs favorably.[21] The decay of Bp$^{\bullet+}$ and recovery of TMB$^{\bullet+}$ can be attributed to the hole transfer from Bp$^{\bullet+}$ to TMB. The observed bimolecular hole-transfer reactions are summarized in eqs 9−12

$$\mathrm{TMB}^{\bullet+} + h\nu_{532} \rightarrow \mathrm{TMB}^{\bullet+}* \quad (9)$$

$$\mathrm{TMB}^{\bullet+}* \rightarrow \mathrm{TMB}^{\bullet+} + h\nu_{\mathrm{f}} \text{ or heat} \quad (10)$$

$$\mathrm{TMB}^{\bullet+}* + \mathrm{Bp} \rightarrow \mathrm{Bp}^{\bullet+} + \mathrm{TMB} \quad (11)$$

$$\mathrm{Bp}^{\bullet+} + \mathrm{TMB} \rightarrow \mathrm{Bp} + \mathrm{TMB}^{\bullet+} \quad (12)$$

An as Q. Similar experimental results were observed for TMB$^{\bullet+}$ and An. The bleaching and complete recovery of the transient absorption of TMB$^{\bullet+}$ at 580 nm were observed upon the second 532-nm laser excitation of TMB$^{\bullet+}$ in the presence of An ($E_{1/2}{}^{ox}$ = +1.76 V vs SCE in acetonitrile)[22,23] as shown in Figure 3 and the inset, indicating the hole transfer from TMB$^{\bullet+*}$ to An to give An$^{\bullet+}$ and subsequent hole transfer from An$^{\bullet+}$ to TMB to give TMB$^{\bullet+}$ (eqs 13 and 14). The absorption of An radical cation (An$^{\bullet+}$) around 445 nm[21] was difficult to observe because of overlap with the absorption of Chl$^{\bullet-}$.

$$\mathrm{TMB}^{\bullet+}* + \mathrm{An} \rightarrow \mathrm{An}^{\bullet+} + \mathrm{TMB} \quad (13)$$

$$\mathrm{An}^{\bullet+} + \mathrm{TMB} \rightarrow \mathrm{An} + \mathrm{TMB}^{\bullet+} \quad (14)$$

Np as Q. The experimental results for Np as Q are shown in Figure 4. During the first 355-nm laser excitation, the growth and decay of the transient absorption were observed at 703 nm (Figure 4a). Because the concentration of Np (0.03−0.30 M) was higher than that of TMB (1.0×10^{-2} M), electron transfer from Np to ^{3}Chl* occurred to give Np$^{\bullet+}$ with the absorption around 703 nm.[21] Subsequent decay of Np$^{\bullet+}$ indicates the hole transfer from Np$^{\bullet+}$ to TMB occurred to give TMB$^{\bullet+}$. However, the absorption at 703 nm did not decay to zero within 100 ns, suggesting that the hole transfer from Np$^{\bullet+}$ to TMB occurs competitively with the other process. It is well known that the dimerization of Np$^{\bullet+}$ with Np gives Np$_2{}^{\bullet+}$,[24−27] which is considered to be a competitive process of hole transfer from Np$^{\bullet+}$ to TMB, because of high concentrations of Np. Because the oxidation potential of Np$_2{}^{\bullet+}$ is expected to be 0.5 V lower than that of Np$^{\bullet+}$ due to the stabilization energy ($-\Delta H$ = $\sim$50 kJ mol^{-1}) of Np$_2{}^{\bullet+}$,[28−30] the hole transfer from Np$_2{}^{\bullet+}$ to TMB is impossible. Because the equilibrium between Np$_2{}^{\bullet+}$ and Np$^{\bullet+}$ exists,[28−30] the remained absorption at 703 nm in the time scale longer than 100 ns should be attributed to the dimerization of Np$^{\bullet+}$ (eqs 15−17)

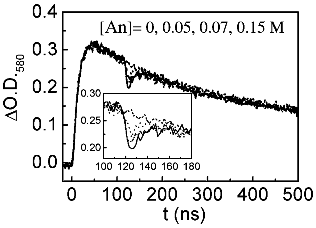

Figure 3. Kinetic traces of ΔO.D.$_{580}$ during the two-color two-laser flash photolysis of a mixture of TMB (1.0×10^{-2} M) and Chl (5.0×10^{-3} M) in aerated acetonitrile in the presence of An (0 (dash line), 0.05 (dot line), 0.07 (dash−dot line), and 0.15 M (solid line)).

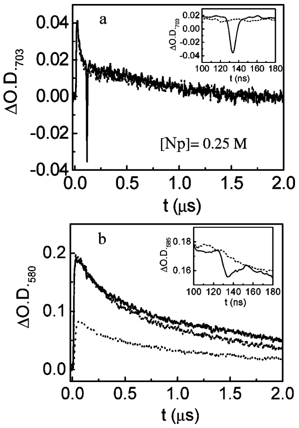

Figure 4. Kinetic traces illustrating the time profiles of ΔO.D.$_{703}$ (a) and ΔO.D.$_{580}$ (b) during the two-color two-laser flash photolysis of a mixture of TMB (1.0×10^{-2} M) and Chl (5.0×10^{-3} M) in aerated acetonitrile in the presence of Np with 0 (dash line) and 0.25 M (solid line). The inset (a) shows the profiles expanded during the second 532-nm laser irradiation. The dot line (b) shows the decay of Np$_2{}^{\bullet+}$ at 580 nm during the 355-nm laser flash photolysis of a mixture of Np (1.0×10^{-2} M) and Chl (5.0×10^{-3} M) in acetonitrile.

$$^3\mathrm{Chl}* + \mathrm{Np} \rightarrow \mathrm{Np}^{\bullet+} + \mathrm{Chl}^{\bullet-} \quad (15)$$

$$\mathrm{Np}^{\bullet+} + \mathrm{TMB} \rightarrow \mathrm{Np} + \mathrm{TMB}^{\bullet+} \quad (16)$$

$$\mathrm{Np}^{\bullet+} + \mathrm{Np} \rightleftharpoons \mathrm{Np}_2{}^{\bullet+} \quad (17)$$

During the second 532-nm laser irradiation, the strong emission at 703 nm was observed (Figure 4a and the inset). Although Np$_2{}^{\bullet+}$ has a weak absorption around 580 nm, no emission from Np$_2{}^{\bullet+}$ in the excited states has been reported.[31,32]

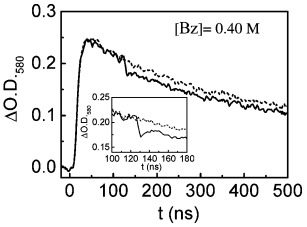

Figure 5. Kinetic traces of ΔO.D.$_{580}$ during the two-color two-laser flash photolysis of a mixture of TMB (1.0×10^{-2} M) and Chl (5.0×10^{-3} M) in aerated acetonitrile in the presence of Bz (0 (dash line) and 0.40 M (solid line)). The inset shows the time profiles expanded during the second 532-nm laser irradiation.

The strong emission at 703 nm is assigned to TMB$^{\bullet+*}$. The bleaching of the transient absorption at 580 nm during the excitation of TMB$^{\bullet+}$ (Figure 4b and the inset) corresponds to the hole transfer from TMB$^{\bullet+*}$ to Np. Although the absorption at 580 nm was completely recovered, the recovery time (∼20 ns) was much shorter than that for Bp or An as Q (∼40 ns). The short recovery time can be attributed to the overlap with the absorption of Np$_2^{\bullet+}$ around 580 nm with the ϵ value ($\epsilon \sim$ 4500 M^{-1}cm^{-1})[24−27] similar to that of TMB$^{\bullet+}$ at 580 nm. Because the lifetime of Np$_2^{\bullet+}$ is different from that of TMB$^{\bullet+}$, the decay at 580 nm during the two-laser flash photolysis became different from that during the single-laser flash photolysis in the microsecond time scale (Figure 4b). The decay of Np$_2^{\bullet+}$ at 580 nm was given in Figure 4b for a comparison.[32] Therefore, the absorption recovery at 580 nm corresponds to both the hole transfer from Np$^{\bullet+}$ to TMB and the dimerization of Np$^{\bullet+}$ with Np to give Np$_2^{\bullet+}$.

Bz as Q. Because the oxidation potential of Bz ($E_{1/2}^{\mathrm{ox}} = +2.3$ V vs SCE in acetonitrile)[22,23] is much higher than that of TMB, the electron-transfer reaction between ^{3}Chl* and Bz is much slower than the electron-transfer reaction between ^{3}Chl* and TMB.[4] However, Bz$^{\bullet+}$ has no absorption at 580 nm.[33,34] Therefore, during the first 355-nm laser irradiation, the transient absorption at 580 nm was attributed to the absorption of TMB$^{\bullet+}$. The bleaching of the transient absorption at 580 nm during the excitation of TMB$^{\bullet+}$ (Figure 5 and the inset) corresponds to the hole transfer from TMB$^{\bullet+*}$ to Bz to give Bz$^{\bullet+}$. However, only a part of bleached TMB$^{\bullet+}$ was recovered. This should be attributed to the dimerization of Bz$^{\bullet+}$ with Bz to give Bz$_2^{\bullet+}$ [33,34] because Bz$_2^{\bullet+}$ does not exhibit absorption at 580 nm. The recovered component of the absorption at 580 nm during the second 532-nm laser excitation was assigned to the hole transfer from Bz$^{\bullet+}$ to TMB to give TMB$^{\bullet+}$ (eqs 18−21)

$$^3\mathrm{Chl}^* + \mathrm{TMB} \rightarrow \mathrm{TMB}^{\bullet+} + \mathrm{Chl}^{\bullet-} \tag{18}$$

$$\mathrm{TMB}^{\bullet+}* + \mathrm{Bz} \rightarrow \mathrm{Bz}^{\bullet+} + \mathrm{TMB} \tag{19}$$

$$\mathrm{Bz}^{\bullet+} + \mathrm{TMB} \rightarrow \mathrm{Bz} + \mathrm{TMB}^{\bullet+} \tag{20}$$

$$\mathrm{Bz}^{\bullet+} + \mathrm{Bz} \rightarrow \mathrm{Bz_2}^{\bullet+} \tag{21}$$

Discussion

Hole Transfer Rate Constant from TMB$^{\bullet+*}$ to Q. Because bleaching of the transient absorption of TMB$^{\bullet+}$ (ΔΔO.D.$_{580}$) and the growth of the transient absorption of Q$^{\bullet+}$ (ΔΔO.D.) increased with increasing the concentration of Q ([Q]), the hole transfer rate constant (k_{ht}) from TMB$^{\bullet+*}$ to Q can be estimated from eq 22[9,10]

$$|\Delta\Delta\mathrm{O.D.}|/\beta = (k_{\mathrm{ht}} \times [\mathrm{Q}])/(k_{\mathrm{IC}} + k_{\mathrm{rad}} + (k_{\mathrm{ht}} \times [\mathrm{Q}])) \tag{22}$$

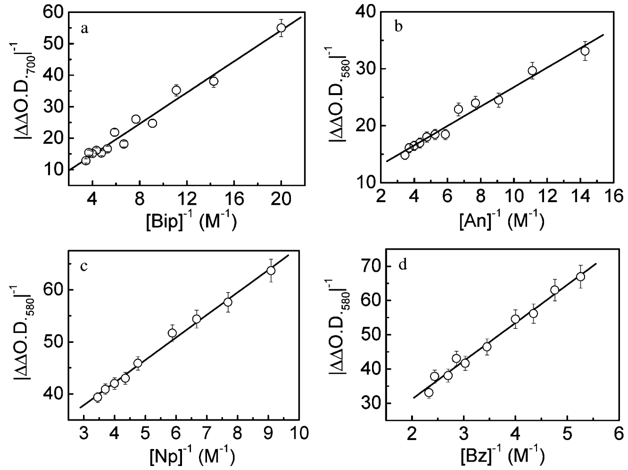

Figure 6. Plots of $|\Delta\Delta\mathrm{O.D.}_{700}|^{-1}$ vs [Bp]$^{-1}$ (a) and plots of $|\Delta\Delta\mathrm{O.D.}_{580}|^{-1}$ vs [An]$^{-1}$ (b), [Np]$^{-1}$ (c), and [Bz]$^{-1}$ (d).

where β refers to a constant indicating a ratio of TMB$^{\bullet+}$ excited during the second 532-nm laser excitation. k_{IC} and k_{rad} refer to the internal conversion (IC) and radiative decay rate from TMB$^{\bullet+}$*, respectively. The plots of $|\Delta\Delta\mathrm{O.D.}_{700}|^{-1}$ versus [Bp]$^{-1}$ and plots of $|\Delta\Delta\mathrm{O.D.}_{580}|^{-1}$ versus [An]$^{-1}$, [Np]$^{-1}$, and [Bz]$^{-1}$ are shown in Figure 6. The linear relationship between $|\Delta\Delta\mathrm{O.D.}|^{-1}$ and [Q]$^{-1}$ was obtained for each case as expected from eq 22.

From the slope and intercept of the linear plots between $|\Delta\Delta\mathrm{O.D.}|^{-1}$ and [Q]$^{-1}$, k_{ht} were estimated to be $(8.5 \pm 0.4) \times 10^{10}$, $(1.4 \pm 0.7) \times 10^{11}$, $(1.3 \pm 0.6) \times 10^{11}$, and $(6.4 \pm 0.3) \times 10^{10}$ M^{-1}s^{-1} for Q as Bp, An, Np, and Bz, respectively, based on the lifetime of TMB$^{\bullet+*}$ ($\tau_{\mathrm{D2}} = 1/(k_{\mathrm{IC}} + k_{\mathrm{rad}}) = 41 \pm 2$ ps).[14] The k_{ht} values were found to be much larger than k_{diff} ($k_{\mathrm{diff}} = 1.9 \times 10^{10}$ M^{-1}s^{-1}, 25 °C) in acetonitrile.[23] This is attributed to the contributions of the lifetime-dependent quenching process or static quenching process during the quenching of TMB$^{\bullet+*}$ by Q, as discussed below.

Hole Transfer Mechanisms from TMB$^{\bullet+*}$ to Q. For the quenching process of the short-lived intermediate by Q of high concentration, Ware and his co-workers proposed a theoretical model consisting of the lifetime-independent and -dependent terms as in eq 23[35]

$$k = k_{\mathrm{diff}} + k_{\mathrm{diff}}\,\sigma'/(\pi D\tau)^{0.5} \tag{23}$$

where $k_{\mathrm{diff}} = 4\pi N\sigma' D$, σ' is the collisional distance between two molecules, D is the sum of the diffusion coefficients for reaction molecules, τ is the lifetime of the excited species, which has serious effect on the k value, and N is the Avogadro number. The contributions of the lifetime-dependent term ($k_{\mathrm{diff}}\sigma'/(\pi D\tau)^{0.5}$) to k_{ht} were calculated to be 78%, 86%, 85%, and 70% for Bp, An, Np, and Bz as Q in acetonitrile, respectively. These results indicate that the static quenching process is the main process in the hole transfer from TMB$^{\bullet+*}$ to Q.

Hole Transfer Rate Constant from Q$^{\bullet+}$ to TMB. In contrast to TMB$^{\bullet+*}$, because Q$^{\bullet+}$ has a long lifetime in the order of microseconds, the contribution of the lifetime-dependent term ($k_{\mathrm{diff}}\sigma'/(\pi D\tau)^{0.5}$) on k is small. Thus, $k'_{\mathrm{ht}} \approx k_{\mathrm{diff}}$. The time scales for the recovery at 580 nm and decay at 700 nm for Bp in Figure 2 and the recovery at 580 nm for An in Figure 3 were almost the same, indicating that the hole transfer from Q$^{\bullet+}$ to TMB to give TMB$^{\bullet+}$ was almost a diffusion-controlled process. Because the concentration of Q$^{\bullet+}$ (∼1.0×10^{-5} M calculated from ΔΔO.D.$_{580}$ and ϵ value of TMB$^{\bullet+}$) produced during the second 532-nm laser irradiation is much lower than that of TMB (1.0

SCHEME 1: Schematic Energy Diagram of $TMB^{\bullet+*}$ ($TMB^{\bullet+}(D_2)$), $TMB^{\bullet+}(D_1)$, and $TMB^{\bullet+}(D_0)$. $h\nu_{532}$, the Second 532-nm Laser Radiation[a]

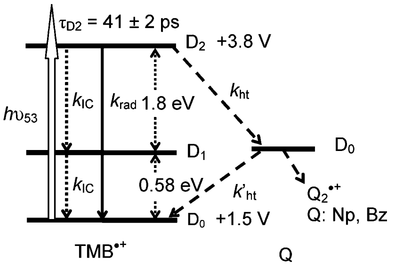

[a] k_{IC}, internal conversion rate constant; k_{rad}, fluorescence rate constant for the $D_2 \rightarrow D_0$ transition; τ_{D2}, D_2 state lifetime. The solid line arrow, the dotted line arrows, and the broken line arrows show the radiative decay, nonradiative decay, and hole transfer or dimerization processes, respectively. The energy gaps were obtained from the ZINDO/S method based on the MO's calculated by the AM1 method.

$\times 10^{-2}$ M), the hole transfer from $Q^{\bullet+}$ to TMB to give $TMB^{\bullet+}$ can be treated as a pseudo-first-order kinetics. From the concentration of TMB and the recovery time scale of the transient absorption at 580 nm, the rate constant (k'_{ht}) of the hole transfer from $Bp^{\bullet+}$ or $An^{\bullet+}$ to TMB was calculated to be $(3.5 \pm 0.2) \times 10^9$ M^{-1} s^{-1}.

Schematic Energy Diagram of $TMB^{\bullet+*}$. The hole-transfer reactions from $TMB^{\bullet+*}$ to Q to give $Q^{\bullet+}$ with k_{ht}, subsequent hole transfer from $Q^{\bullet+}$ to TMB to give $TMB^{\bullet+}$ with k'_{ht} or dimerization between $Q^{\bullet+}$ and Q to give $Q_2^{\bullet+}$, and the calculated energy gaps of the $D_0-D_1-D_2$ states are shown in Scheme 1.[14,18]

Because the calculated oscillator strength for the $D_1 \leftarrow D_0$ and $D_2 \leftarrow D_0$ transitions were 0.0003 and 0.0508, respectively,[18,37] the transition of $D_1 \leftarrow D_0$ is essentially a forbidden process. The fluorescence of $TMB^{\bullet+*}$ corresponds to the $D_2 \rightarrow D_0$ transition of $TMB^{\bullet+}$ was confirmed.[14,18,36] During the second 532-nm laser excitation of $TMB^{\bullet+}(D_0)$, $TMB^{\bullet+*}$ ($TMB^{\bullet+}(D_2)$) was produced with $\tau_{D_2} = 41 \pm 2$ ps).[14] In the presence of Q such as Bp, An, Np, and Bz, hole transfer from $TMB^{\bullet+*}$ to Q to give $Q^{\bullet+}$ occurs. Because the oxidation potential of Q is higher than that of TMB, the subsequent hole transfer from $Q^{\bullet+}$ to TMB to give $TMB^{\bullet+}$ occurs. When Q is an aromatic hydrocarbon such as Np or Bz, the dimerization between $Q^{\bullet+}$ and Q to give $Q_2^{\bullet+}$ competitively occurs with the hole transfer from $Q^{\bullet+}$ to TMB to give $TMB^{\bullet+}$.

Conclusions

Bimolecular hole transfer from $TMB^{\bullet+*}$ to Q to give $Q^{\bullet+}$ and subsequent hole transfer from $Q^{\bullet+}$ to TMB to give $TMB^{\bullet+}$ were directly observed during the two-color two-laser flash photolysis at room temperature. In the case of Bp as Q, the growth and decay of the transient absorption of $Bp^{\bullet+}$ at 700 nm together with the bleaching and complete recovery of the transient absorption of $TMB^{\bullet+}$ at 580 nm were observed. In the case of An, Np, and Bz as Q, the bleaching of the transient absorption of $TMB^{\bullet+}$ at 580 nm was observed. The k_{ht} was estimated to be $(8.5 \pm 0.4) \times 10^{10}$, $(1.4 \pm 0.7) \times 10^{11}$, $(1.3 \pm 0.6) \times 10^{11}$, and $(6.4 \pm 0.3) \times 10^{10}$ $M^{-1}s^{-1}$ for Q as Bp, An, Np, and Bz in acetonitrile, respectively, indicating the importance of a lifetime-dependent process in hole transfer from $TMB^{\bullet+*}$ to Q. Alternatively, the hole transfer from $Bp^{\bullet+}$ or $An^{\bullet+}$ to TMB to give $TMB^{\bullet+}$ occurred at $(3.5 \pm 0.2) \times 10^9$ M^{-1} s^{-1} in acetonitrile, indicating the diffusion-controlled process. Whereas, for Q as NP and Bz, dimerization of $Q^{\bullet+}$ with Q to give $Q_2^{\bullet+}$ occurred competitively with hole transfer from $Np^{\bullet+}$ or $Bz^{\bullet+}$ to TMB.

Acknowledgment. This work has been partly supported by a Grant-in-Aid for Scientific Research (Project 17105005, Priority Area (417), 21st Century COE Research, and others) from the Ministry of Education, Culture, Sports, Science and Technology (MEXT) of Japanese Government. We also thank to JSPS for a fellowship for X.C.

References and Notes

(1) Fox, M. A. *Chem. Rev.* **1979**, *79*, 253.
(2) Julliard, M.; Chanon, M. *Chem. Rev.* **1983**, *83*, 425.
(3) Breslin, D. T.; Fox, M. A. *J. Phys. Chem.* **1994**, *98*, 408.
(4) Kavarnos, G. J.; Turro, N. J. *Chem. Rev.* **1986**, *86*, 401.
(5) Cook, A. R.; Curtiss, L. A.; Miller, J. R. *J. Am. Chem. Soc.* **1997**, *119*, 5729.
(6) Gosztola, D.; Niemczyk, M. P.; Svec, W.; Lukas, A. S.; Wasielewski, M. R. *J. Phys. Chem. A* **2000**, *104*, 6545.
(7) Eriksen, J.; Joergensen, K. A.; Linderberg, J.; Lund, H. *J. Am. Chem. Soc.* **1984**, *106*, 5083.
(8) Wang, Z.; McGimpsey, W. G. *J. Phys. Chem.* **1993**, *97*, 5054.
(9) Ishida, A.; Fukui, M.; Ogawa, H.; Tojo, S.; Majima, T.; Takamuku, S. *J. Phys. Chem.* **1995**, *99*, 10808.
(10) Majima, T.; Fukui, M.; Ishida, A.; Takamuku, S. *J. Phys. Chem.* **1996**, *100*, 8913.
(11) Fujita, M.; Ishida, A.; Majima, T.; Takamuku, S. *J. Phys. Chem.* **1996**, *100*, 5382.
(12) Okhrimenko, A. N.; Gusev, A. V.; Rodgers, M. A. J. *J. Phys. Chem. A* **2005**, *109*, 7653.
(13) Pages, S.; Lang, B.; Vauthey, E. *J. Phys. Chem. A* **2006**, *110*, 7547.
(14) Cai, X.; Sakamoto, M.; Fujitsuka, M.; Majima, T. *Chem. Phys. Lett.* **2006**, *432*, 436.
(15) Cai, X.; Sakamoto, M.; Hara, M.; Tojo, S.; Ouchi, A.; Sugimoto, A.; Kawai, K.; Endo, M.; Fujitsuka, M.; Majima, T. *J. Phys. Chem. A* **2005**, *109*, 3797.
(16) Gschwind, R.; Haselbach, E. *Helv. Chim. Acta* **1979**, *62*, 941.
(17) Hilinski, E. F.; Milton, S. V.; Rentzepis, P. M. *J. Am. Chem. Soc.* **1983**, *105*, 5193.
(18) Ichinose, N.; Tanaka, T.; Kawanishi, S.; Suzuki, T.; Endo, K. *J. Phys. Chem. A* **1999**, *103*, 7923.
(19) Ichinose, N.; Tanaka, T.; Kawanishi, S. i.; Majima, T. *Chem. Phys. Lett.* **2000**, *326*, 293.
(20) Shida, T.; Iwata, S. *J. Am. Chem. Soc.* **1973**, *95*, 3473.
(21) Shida, T. *Electronic Absorption Spectra of Radical Ions*; Elsevier Science Publishers Inc.: Tokyo, 1988.
(22) Meites, L.; Zuman, P. *CRC Handbook Series in Organic Electrochemistry*; CRC Press, Inc.: Cleveland, OH, 1976; Vol. I.
(23) Murov, S. L.; Carmichael, I.; Hug, G. L. *Handbook of Photochemistry*; Marcel Dekker, Inc.: New York, 1993.
(24) Kira, A.; Imamura, M. *J. Phys. Chem.* **1979**, *83*, 2267.
(25) Kira, A.; Imamura, M.; Shida, T. *J. Phys. Chem.* **1976**, *80*, 1445.
(26) Tsuchida, A.; Tsujii, Y.; Ito, S.; Yamamoto, M.; Wada, Y. *J. Phys. Chem.* **1989**, *93*, 1244.
(27) Tsuchida, A.; Yamamoto, M.; Nishijima, Y. *J. Phys. Chem.* **1984**, *88*, 5062.
(28) Inokuchi, Y.; Ohashi, K.; Matsumoto, M.; Nishi, N. *J. Phys. Chem.* **1995**, *99*, 3416.
(29) Fushimi, T.; Fujita, Y.; Ohkita, H.; Ito, S. *J. Photochem. Photobiol., A* **2004**, *165*, 69.
(30) Fushimi, T.; Fujita, Y.; Ohkita, H.; Ito, S. *Bull. Chem. Soc. Jpn.* **2004**, *77*, 1443.
(31) Saigusa, H.; Lim, E. C. *J. Phys. Chem.* **1994**, *98*, 13470.
(32) Cai, X.; Tojo, S.; Fujitsuka, M.; Majima, T. *J. Phys. Chem. A* **2006**, *110*, 9319.
(33) Kochi, J. K.; Rathore, R.; Le Magueres, P. *J. Org. Chem.* **2000**, *65*, 6826.
(34) Todo, M.; Okamoto, K.; Seki, S.; Tagawa, S. *Chem. Phys. Lett.* **2004**, *399*, 378.
(35) Andre, J. C.; Niclause, M.; Ware, W. R. *Chem. Phys.* **1978**, *28*, 371.
(36) Ichinose, N.; Majima, T. *Chem. Phys. Lett.* **2000**, *322*, 15.